Gibbs ringing removal in diffusion MRI using second order total variation minimization

Jelle Veraart[1], Florian Knoll[1], Jan Sijbers[2], Els Fieremans[1], and Dmitry S. Novikov[1]

[1]*Center for Biomedical Imaging, NYU Langone Medical Center, New York, NY, United States,* [2]*iMinds - Vision Lab, University of Antwerp, Antwerp, Belgium*

TARGET AUDIENCE: Researchers interested in diffusion MRI processing and microstructural modeling.

PURPOSE: **To remedy strong bias on diffusion metrics due to the Gibbs ringing artifact.** MR images are affected by the Gibbs ringing that appears near sharp edges, due to truncation of the k-space. While introducing a bias of maximally 9% in the weighted images, the Gibbs effect is amplified tremendously in the derived parametric maps, e.g. of diffusion and kurtosis tensor components. The amplification occurs because the Gibbs oscillations in the b=0 and finite-b images are out of phase due to relative difference in DW signal, $S(b)$, intensities at different b-values. Fig. 1 shows this for realistic values on the CSF-Corpus Callosum border with diffusion and kurtosis estimated in the radial direction. This creates a *concave*, rather than convex, log $S(b)$, leading to extreme unphysical ADC and AKC values. Practically, the fits hit the physically expected bounds (e.g. positive diffusivity and kurtosis), resulting in the "black voxels", Fig. 4a, where these parameters cannot be estimated. So far, the Gibbs ringing bias is ignored or reduced by isotropic smoothing at the expense of spatial resolution loss and the introduction of partial volume effects. **Here we demonstrate that extrapolating the data in k-space beyond the maximally measured k_c by means of second order total generalization variation[1] (TGV) minimization substantially reduces Gibbs ringing and noise of the MRI data without compromising resolution**.

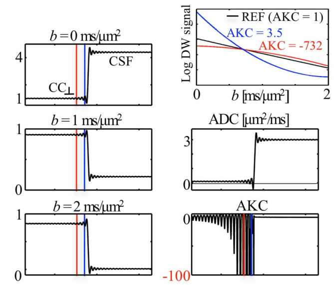

Fig. 1: The over- and undershoots of the ADC and AKC largely exceeds the 9% that has been observed on the diffusion MR signals, and can result in extreme physically implausible values, typically observed as "black voxels" (Fig. 4a)

METHODS: The basic idea is to extrapolate, at least partially, the k-space data truncated beyond the k-space edge k_c, in order to better define the signal intensity near the edges. Inspired by concepts of Compressed Sensing and earlier work[2,3], we formulate the extrapolation of the k-space as a regularized minimization problem $\hat{u} = \arg\min_u \|\tilde{\mathcal{F}}u - \tilde{k}\|_2^2 + \lambda\mathcal{R}(u)$. Here the 1st term preserves the fidelity with the acquired data $\tilde{k}$ ($\tilde{\mathcal{F}}$ is the windowed Fourier transformation), and the penalty term $\mathcal{R}(u)$ is based on the L_1 norm of the image u in the basis where it is presumed to be sparse, with a regularization parameter λ chosen according to the discrepancy criteria[4]. Of course, the challenge is to find the "right" sparse basis. In this work we evaluate the second order TGV function[5]: $\mathcal{R}(u) = \arg\min_v 2\int_\Omega \|\nabla u - v\|_1\,\mathrm{d}x + \int_\Omega \|\nabla v\|_1\,\mathrm{d}x$ where v is a 2-dimensional vector field within a slice, bounded by 0 and ∇u, and compare it to the more commonly used total variation (TV) [2,3]. Unlike TV, the second order TGV sparsifies piecewise linear functions. **The reduced penalty term for this non-constant linear functions avoids the *staircasing* effect**, which is often observed in TV regularization. The primal dual algorithm was used to solve the optimization problem[6]. Zero-filled (ZF) solutions with and without filtering (Lanczos and Gaussian) were calculated for comparison.

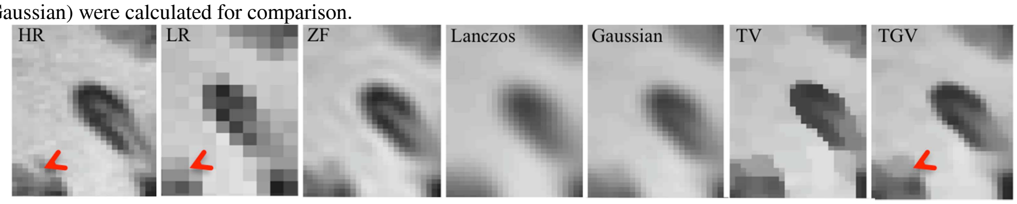

Fig. 2: Reconstructions MPRAGE image of the periventricular white matter. TGV outperforms all others since it features (I) high resolution (v. filtering), (II) full suppression of Gibbs ringing (v. Gaussian filtering) and (III) the absence of the staircasing artifact (v. TV).

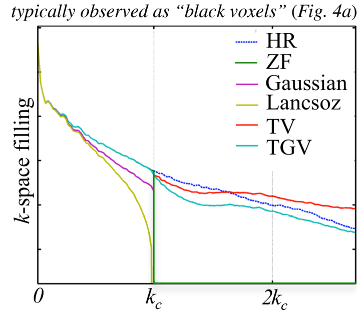

Fig. 3: k-space energy density as function of the distance to the k-space center. TGV closely approximates the HR data, whereas TV overshoots the high frequency content (cf. staircasing artifact, see Fig. 2). Windowing filtering destroys measurements resulting in spatial resolution loss. Note broad peak at $2k_c$.

RESULTS:

A. Structural MRI: Truncating a high-resolution (HR; 256x256) MPRAGE image in k-space (cut-off frequency k_c) generated a simulated image that mimics a low-resolution "acquisition" (LR; 96x96). A qualitative comparison of the different filtering and reconstruction techniques, i.e. zero-filling (ZF), TV, and TGV, applied on the single slice of a simulated image shows that Gibbs ringing can be strongly reduced by extrapolation of the k-space using second order TGV without the introduction of the staircase or loss of spatial resolution compared to LR acquisition (Fig. 2). However, fine anatomical details lost during LR acquisition cannot be recovered (see red arrows). This is expected, as we are not randomly sampling in the HR k-space (for the compressed sensing reconstruction to work). However, we are not aiming to resolve all HR details, only to cure the ringing artifact. Both the Lanczos and Gaussian filters show significant spatial resolution loss. The corresponding k-space filling, i.e. the k-energy density as function of the distance to the k-space center shows that **in contrast to window filtering, both TV and TGV hardly affect the actually measured k-space data, $k<k_c$** (Fig. 3). We observe good recovery of k-space filling beyond k_c for both TV and TGV. The broad peak at $k\sim2k_c$ is a signature of the nonlinear reconstruction (harmonic doubling). TV's *overestimation* of high frequencies compared to the HR data explains the *staircase* artifact observed in the corresponding image, as it models the image as a piecewise constant function[2,3]. The TGV reconstructed images do not show the staircase artifacts.

B. Diffusion MRI: Fig. 4 shows mean kurtosis (MK; a-d) and axonal water fraction[7] (AWF; e-h) maps of a detail, i.e. the splenium, of a single axial slice of the Human Connectome Project (HCP) data, which was downsampled to 96x96 by truncation of the k-space and subsequently reconstructed to the original 144x174 resolution using ZF, TV, and TGV. Without smoothing and constraining the kurtosis tensor fit, extreme negative MK values ("black voxels") and/or unexpected heterogeneity in AWF are observed in regions of interest such as the Corpus Callosum. (a). Current practice is to smooth and constraint the data fit (b, f). **Both TV (c, g) and TGV (d, h) result in a more robust fit as they minimize the Gibbs effect and the noise without manipulation of the resulting statistics and loss of spatial resolution.**

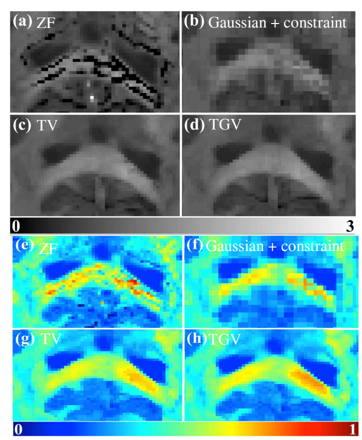

Fig. 4: Detail of MK (a-d) and AWF (e-h) of an axial slice of HCP data. The MK maps often show black voxels in the splenium, indicating outliers in the kurtosis fit. The quality of the maps improves significantly with the proposed technique. Note the heterogeneity of (b,f) compared to (c,g) and (d,h).

DISCUSSION & CONLUSION: We obtain promising results in suppressing the Gibbs artifact by extrapolation k-space data beyond the measurements by means of second order TGV minimization. The second order TGV framework inherently assumes that the underlying MR data can be modeled by a piecewise linear function. However, since the extrapolation of the k-space is solely based on that model assumption, fine anatomical details that are concealed in the unmeasured part of the k-space might not be recovered. Full recovery would require at least a random sampling of the k-space, including the high frequencies (cf. Compressed Sensing theory). Nonetheless, we showed that diffusion and kurtosis tensor elements are estimated more robustly and accurately, i.e. without violating physical constraints, using the TGV-based Gibbs correction. Moreover, unlike filtering techniques, the proposed framework hardly affects the actually measured k-space data ($k<k_c$) and, as such, maintains the acquisition resolution. The maps of derived microstructural parameters are smooth and have expected physical values.

Work supported by NIH R01 NS088040 and Interuniversity Attraction Poles Program (P7/11) initiated by the Belgian Science Policy Office

REFERENCES: [1]Knoll et al. MRM 65:480(2011) [2]Block et al. Int. J. of Biomed. Imag.: ID 184123 (2008) [3]Perrone et al. 4th ISMRM Benelux Chapter, p. 99 (2012) [4]Hunt IEEE Trans Comput 22:805(1973) [5]Bredies et al. SIAM J Imaging Sci 3:492 (2010) [6]Chambolle et al. of Math Imag and Vision 40:120(2010) [7]Fieremans et al. NeuroImage 58:177 (2011)